ARTICLE IN PRESS

Solid State Electronics xxx (xxxx) xxx–xxx

Contents lists available at ScienceDirect

Solid State Electronics

journal homepage: www.elsevier.com/locate/sse

Effect of oxygen content of the $LaAlO_3$ layer on the synaptic behavior of Pt/$LaAlO_3$/Nb-doped $SrTiO_3$ memristors for neuromorphic applications

Jun Tae Jang[a], Daehyun Ko[a], Geumho Ahn[a], Hye Ri Yu[a], Haesun Jung[a], Yeon Soo Kim[b], Chansoo Yoon[b], Sangik Lee[b], Bae Ho Park[b], Sung-Jin Choi[a], Dong Myong Kim[a], Dae Hwan Kim[a,*]

[a] School of Electrical Engineering, Kookmin University, 77 Jeongneung-ro, Seongbuk-gu, Seoul 02707, Republic of Korea
[b] Department of Physics, Konkuk University, 120 Neungdong-ro, Gwangjin-gu, Seoul 05029, Republic of Korea

A R T I C L E I N F O

Keywords:
Pt/$LaAlO_3$/Nb-doped $SrTiO_3$ memristor
Synaptic behavior
Thermionic emission
Poole-Frenkel (P-F) emission
Oxygen-content effect
Spike time-dependent plasticity (STDP)

A B S T R A C T

We report the effect of the oxygen content of the $LaAlO_3$ layer on the synaptic behavior in the Pt/$LaAlO_3$/Nb-doped $SrTiO_3$ memristor for neuromorphic applications. As the oxygen-content decreases, the current becomes larger and the spike time-dependent plasticity (STDP) becomes less sensitive to the time difference between pre- and post-synaptic spike voltage. In addition, the conduction mechanism, which was found to be a combination of thermionic and Poole-Frenkel emissions, and the effect of oxygen content are explained in association with the oxygen vacancy in the $LaAlO_3$ layer. The trade-off between large current and efficient STDP can be controlled by the oxygen content. Furthermore, the results of extracting the synaptic strength-based model parameters indicate that the Pt/$LaAlO_3$/Nb-doped $SrTiO_3$ shows the efficient STDP characteristics in comparison to previously reported memristor materials.

1. Introduction

With regard to a diverse oxide-based combined structure, the heterostructures of perovskite oxides are emerging as one of the most fascinating materials with a broad spectrum of functional properties such as two-dimensional electron gas, orbital reconstruction, interfacial superconductivity, ferromagnetism, charge writing, resistive switching (RS), giant thermoelectric effect, and colossal ionic conductivity [1–3]. In particular, the high-mobility characteristics at the interface between two perovskite materials have been frequently observed via intensive experimental and theoretical investigations on the physics such as built-in electric field [4], oxygen vacancy (V_O) migration [5], and cation intermixing [6]. Thus, many researchers have focused bulky and/or interfacial characteristics of the perovskite materials due to various functional features. Applications based on these characteristics have been reported such as the transparent devices using the wide bandgap [7], the nonvolatile memory with the capacitor-like structure [8], and the sensor of the gas responding the palladium nanoparticles [9].

On the other hand, neuromorphic computing to mimic the brain system has been studied to verify low power and high speed device beyond Von Neumann computing system by many researchers [10–12]. In particular, they have developed the device to emulate the neuromorphic computing system where the synapse is a structure that passes an electrical or chemical signal between neuron pair in the nervous system. The one of the devices to emulate these neuromorphic systems is the memristor which enables the bias/time-dependent gradual resistive switching (RS) and is composed of simple metal/insulator/metal structure such as $Pr_{0.7}Ca_{0.3}MnO_3$ [13], Ta_2O_5 [14], γ-Fe_2O_3 [15], amorphous InGaZnO [11,16], and perovskite oxide such as $LaAlO_3$/$SrTiO_3$, $BiFeO_3$/Nb-doped $SrTiO_3$, and amorphous $SrTiO_3$ [7,8,17,18].

Therefore, the synaptic behavior of perovskite materials-based memristor needs to be investigated and assessed in viewpoint of the feasibility of neuromorphic system. In real, perovskite materials-based memristors have attracted much attention as the RS devices. As previously reported, perovskite oxide materials-based memristors showed the RS characteristics between a low resistance state (LRS) and a high resistance state (HRS) associated with the generation of oxygen vacancies (V_Os) which is based on the transition from Ti^{4+} to Ti^{3+} in the $SrTiO_3$ bulk [17].

In this work, we investigate the synaptic behavior in Pt/$LaAlO_3$/Nb-doped $SrTiO_3$ memristor. First of all, we reveal the conduction mechanism of the Pt/$LaAlO_3$/Nb-doped $SrTiO_3$ memristor by modifying the current-voltage (I-V) characteristics. Secondly, we demonstrate the spike time-dependent plasticity (STDP) features to mimic the brain system and analyze the effect of the oxygen-content in the $LaAlO_3$ layer on STDP. Finally, the STDP characteristics are quantized and compared with the previously reported results.

* Corresponding author.
E-mail address: drlife@kookmin.ac.kr (D.H. Kim).

http://dx.doi.org/10.1016/j.sse.2017.10.032

0038-1101/ © 2017 Elsevier Ltd. All rights reserved.

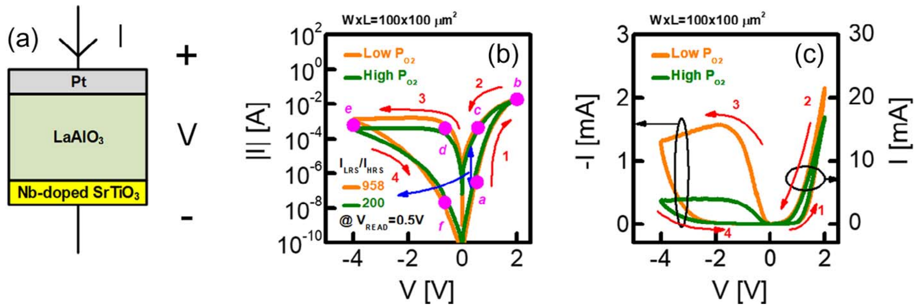

Fig. 1. (a) Device structure and P_{O2}-dependent RS I-V behaviors of (b) log and (c) linear scale in the Pt/$LaAlO_3$/Nb-doped $SrTiO_3$ memristor.

2. Device fabrication and measurement setup

The Pt/$LaAlO_3$/Nb-doped $SrTiO_3$ memristors were fabricated as shown in Fig. 1(a). The Nb-doped $SrTiO_3$ was prepared as the conductive substrate [19,20], which plays the role of bottom electrode (BE). Then, the $LaAlO_3$ was grown as the RS layer by the molecular beam epitaxy at 640 °C on the TiO_2-terminated Nb-doped $SrTiO_3$ substrate. It is known that the Nb-doped $SrTiO_3$ is a very good substrate due to a small lattice mismatch with $LaAlO_3$. It is very useful when one characterizes physical properties of the epitaxial $LaAlO_3$ in the out-of-plane direction. The oxygen-poor and oxygen-rich samples were fabricated by varying the oxygen partial pressure (P_{O2}) from 10^{-6} and 10^{-4} Torr, respectively. The P_{O2} controls the concentration of V_Os in RS film during the $LaAlO_3$ growth. The thickness of $LaAlO_3$ is 7.726 nm, which corresponds to the 20 unit cells. Finally, the 100 nm-thick Pt was deposited as top electrode (TE) with the area of $100 \times 100\,\mu m^2$ by using the dc magnetron sputtering with the power of 50 W.

In order to analyze the electrical characteristics, the dc current-voltage (I-V) and potentiation/depression pulse characteristics were measured at a room temperature and dark condition with Keithley-4200 semiconductor characterization system.

3. Bipolar resistive switching and memristive characteristics

The RS I-V behaviors of the Pt/$LaAlO_3$/Nb-doped $SrTiO_3$ memristors are shown in Fig. 1(b) and (c). The sequence of applying voltage is 0 V → +2 V (SET process) → 0 V → −4 V (RESET process) → 0 V, where both the polarity of voltage and the direction of current flow are shown in Fig. 1(a). The SET process is the RS from a high-resistance state (HRS) to a low-resistance state (LRS) and the RESET process is the RS from LRS to HRS. The I-V hysteresis loop in Fig. 1(b) and (c) shows a stable bipolar RS characteristic. In Fig. 1(b), the point from *a* to *f* indicates a specific operation point. The current ratio of LRS to HRS (I_{LRS}/I_{HRS}) at read voltage (V_{READ}) = 0.5 V is 958 and 200 in the oxygen-poor and oxygen-rich sample, respectively. The voltage polarity of SET/RESET is opposite to previous work [7], where V_Os are supplied from the $SrTiO_3$ bulk, because in our case the initial density of V_Os is quite high due to relatively low P_{O2} during the $LaAlO_3$ deposition. Consistently, it was found by the XPS analysis that the oxygen concentration in $LaAlO_3$ can be controlled by modulating the oxygen partial pressure [21].

The conduction mechanism is somewhat complicated and needs to be fully understood especially in memristive devices because it is dependent on a history of I-V operation. Fig. 2 elucidates the transport mechanism and illustrates it at individual operation point (*a*–*f*). For HRS at a low V_{READ} (the voltage conditions lower than *a* in Fig. 2(a) and lower than *f* in Fig. 2(c)), the conduction follows the thermionic emission:

$$I = AA^{*}T^{2}\exp\left(-\frac{q\phi_B}{kT}\right)\exp\left(\frac{qV}{\eta kT}\right) \tag{1}$$

where the I is the current, A is the area of device, A^* is the Richardson constant, kT is the thermal energy, Φ_B is the effective barrier height, q is the electron charge, and η is the ideality factor. The extracted Φ_B is 0.77 eV and 0.72 eV for the oxygen-poor and oxygen-rich devices, respectively.

For either the HRS at a high V_{READ} (the voltage conditions higher than *a* in Fig. 2(b) and higher than *f* in Fig. 2(d)) or the LRS at a higher/lower V_{READ} than *c*/*d* in Fig. 2(b)/(d), the conduction is dominated by the Poole-Frenkel (P-F) emission:

$$I = AqN_C\mu E\exp\left(-\frac{q\phi_B}{kT}\right)\exp\left(\frac{q}{\eta kT}\sqrt{\frac{qE}{\pi\varepsilon}}\right) \tag{2}$$

where N_C is the density of states in the conduction band, μ is the carrier mobility, ε is the permittivity of the dielectric constant, and E is the electric field. The P-F emission is a means by which electrons with enough energies that can overcome the energy barrier can escape the localized states after the electrons are generally trapped in the localized states, in other words, the P-F mechanism is the continuative hopping phenomenon. The Φ_B for P-F emission is extracted to 0.5 eV and 0.56 eV for the oxygen-poor and oxygen-rich samples, respectively. According to Mitra et al. [22], V_Os in the $LaAlO_3$ can be formed within a variety of ranges of charge state and energy level, such as neutral $V_O{}^0$ (E_C − 2.19 eV), $V_O{}^+$ (E_C − 1.44 eV), and $V_O{}^{2+}$ (E_C − 0.62 eV). In particular, since the V_Os near the E_C of the $LaAlO_3$ layer, which determine the rate of electron migration, have positive charge, the energy barrier lowering due to the positively charged V_Os may occur. Therefore, lower Φ_B in the case of higher density of V_Os (oxygen-poor sample) suggests that the RS characteristic in Pt/$LaAlO_3$/Nb-doped $SrTiO_3$ memristor results from the hopping and migration via V_Os in the $LaAlO_3$ layer. Lower Φ_B in the case of higher density of V_Os (oxygen-poor sample) suggests that the RS characteristic in Pt/$LaAlO_3$/Nb-doped $SrTiO_3$ memristor results from the hopping and migration via V_Os in the $LaAlO_3$ layer.

The memristive behavior is then characterized by the potentiation/depression pulse measurement with the duration of SET/RESET pulse (t_{SET}/t_{RESET}) = 1 ms, the SET/RESET voltage (V_{SET}/V_{RESET}) = +2 V/−2 V, and 50 cycles. The read current (I_{READ}) is sampled during the read period (V_{READ} = 0.5 V) which is inserted between adjacent potentiation/depression pulse trails (Fig. 3(a)). The measured I_{READ} with the increase of the number of cycles is observed as shown in Fig. 3(b). In comparison with the oxygen-rich sample, the oxygen-poor sample shows a higher current and larger difference between the potentiation and depression. Our results suggest that the higher V_O density (oxygen-poor condition) is advantageous in terms of the memristive viewpoint because not only the magnitude of current but also the change of current for the potentiation and depression is very important to obtain the properties of analog memory associated with synaptic behavior and improve the operating speed.

4. Spike time-dependent plasticity characteristics for neuromorphic applications

Nervous system between the axon and dendrite follows the role of memory in the following mechanisms. The ends of the axon and the dendrite are applied to the pre- and post-synaptic spike (V_{pre} and V_{post}),

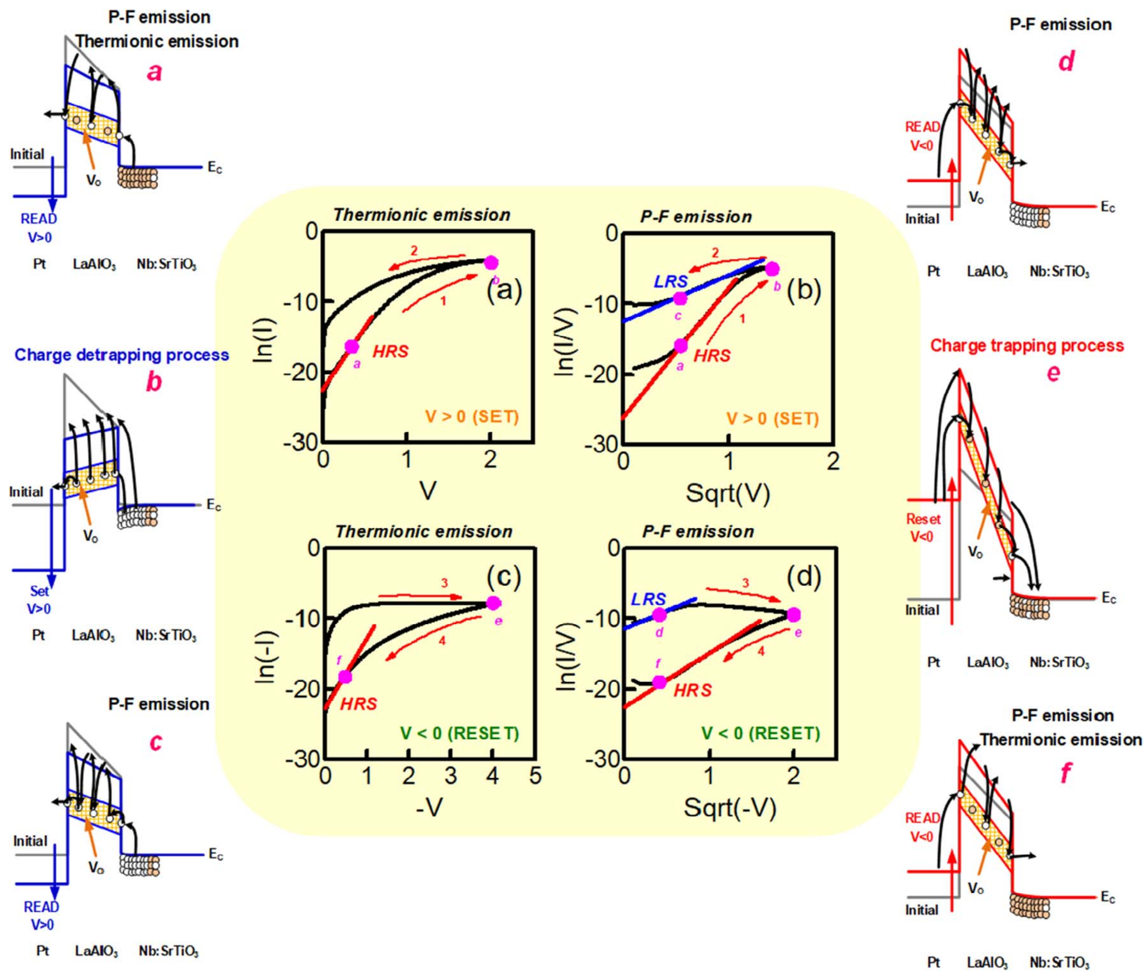

Fig. 2. Conduction mechanism expected by modifying the I-V characteristics in condition of (a), (b) $V > 0$ and (c), (d) $V < 0$; (a), (c) thermionic emission, (b), (d) Poole-Frenkel emission. (*a–f*) illustration of expected transport mechanism at individual operation point.

respectively as shown in the Fig. 4(a). The time difference (Δt) between the two spikes controls the consecutive strength of connectivity, i.e., synaptic weight, which is the rule of STDP. If the Δt between the V_{pre} and V_{post} is considerably short, the synapse is instantaneously applied by the significant higher spike. The neurotransmitters in the synaptic vesicle transfer to information from the end of the axon to the synaptic cleft due to the effectively strong voltage applied to the synapse. And then, when the neurotransmitters activate the receptor in synaptic cleft, the connection between the two neurons is strengthened. Finally, the synapse can remember the information by the applied spikes.

The role of memory in the synapse is very similar to the characteristics for the conductance variation in the memristors. In order to emulate this situation, we designed the V_{pre} and V_{post} and applied them to TE and BE respectively, as depicted in Fig. 4(b). The V_{READ} in the

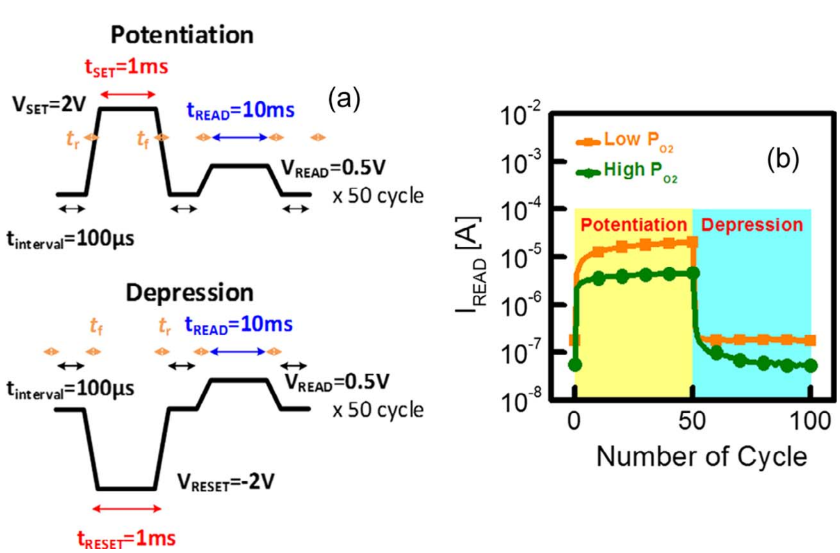

Fig. 3. (a) Measurement conditions and (b) electrical characteristics of the potentiation/depression pulse trails in the Pt/$LaAlO_3$/Nb-doped $SrTiO_3$ memristor with the low and high P_{O2} in the $LaAlO_3$ layer.

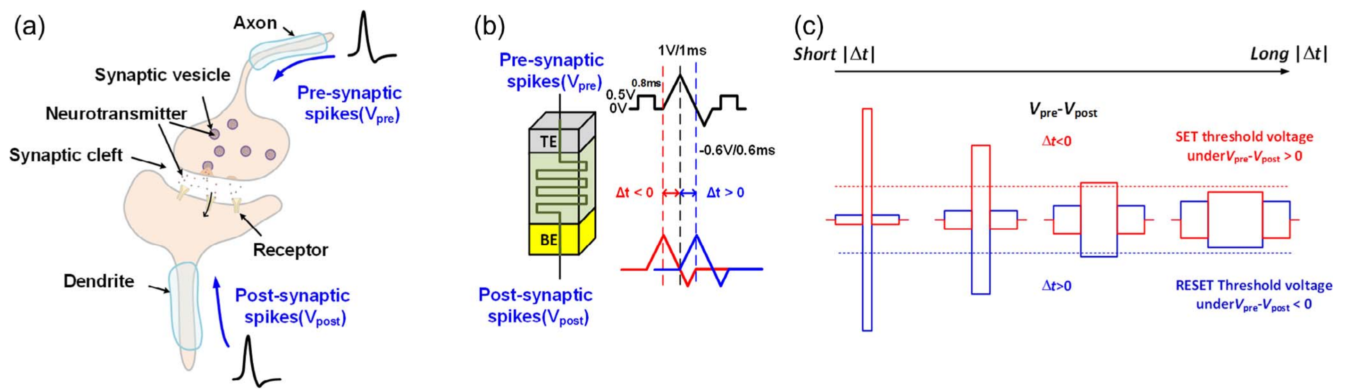

Fig. 4. (a) Nervous system consisting of the axon and dendrite and (b) the memristor device that can mimic the system. (c) The voltage spike difference (V_{pre}-V_{post}) with the time difference (Δt) generated by the voltage spike applied across the memristor.

read region is applied to 0.5 V to check the conductance variation. When the two electrodes in memristor is applied by the synaptic spikes, the maximum voltage across the memristor is changed with the Δt as illustrated in Fig. 4(c). As a results, the conductance of memristor is gradually controlled by Δt, which is the essential STDP function.

The STDP characteristics is represented by the synaptic weight (ΔW) versus Δt. Here, the ΔW is defined by

$$\Delta\ W = \frac{I_{READ,post} - I_{READ,pre}}{I_{READ,pre}} = \frac{\Delta I_{READ}}{I_{READ,pre}}\ [\%], \tag{3}$$

where the $I_{READ,pre}$ and $I_{READ,post}$ are the pre- and post-synaptic I_{READ} and the ΔI_{READ} is difference between $I_{READ,pre}$ and $I_{READ,post}$. Based on the experimental setup, we investigate the STDP characteristics applying the V_{ppre} and V_{post} to verify the feasibility of artificial neuromorphic system based on Pt/$LaAlO_3$/Nb-doped $SrTiO_3$ memristors. The measured ΔI_{READ} and ΔW as a function of Δt are shown as the symbols in Fig. 5. It is found that the ΔI_{READ} is lower and the ΔW is higher in oxygen-poor sample compared with oxygen-rich sample. Our results indicate that the STDP becomes less efficient as the electrons are harder to migrate via V_Os in $LaAlO_3$ layer, as illustrated in Fig. 6.

In addition, the STDP efficiency is quantified according to the synaptic strength-based model [23], where the STDP characteristics are expressed by the two exponential functions:

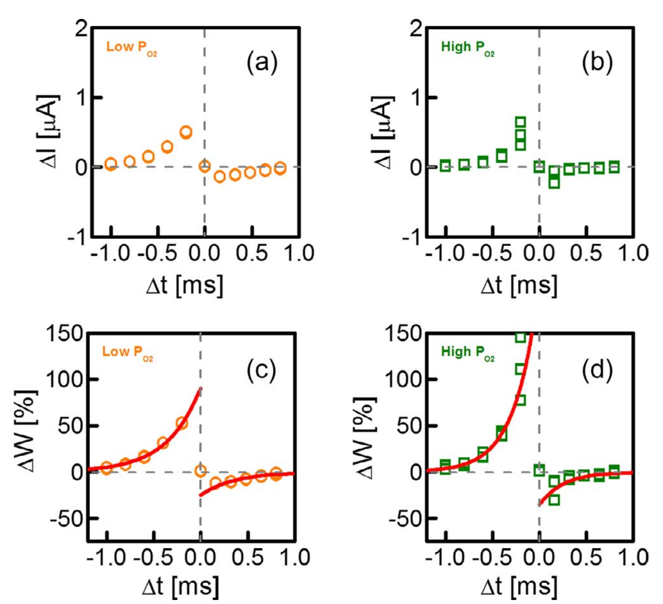

Fig. 5. (a), (b) Current difference (ΔI) and (c), (d) synaptic weight (ΔW) with the time difference (Δt) in the Pt/$LaAlO_3$/Nb-doped $SrTiO_3$ memristor with the (a), (c) low P_{O2} and (b), (d) high P_{O2} in the $LaAlO_3$ layer.

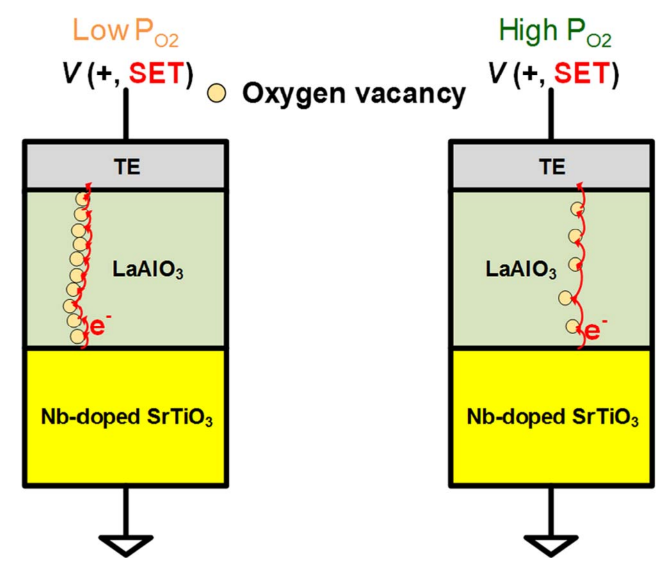

Fig. 6. V_O distribution in the Pt/$LaAlO_3$/Nb-doped $SrTiO_3$ memristor with the P_{O2} in the $LaAlO_3$ layer.

$$\Delta\ W = \Delta W_{0-} \times \exp\left(-\left(\frac{\Delta t}{\tau_-}\right)\right)\ [\%]\ (\Delta\ t< 0), \tag{4}$$

$$\Delta\ W = \Delta W_{0+} \times \exp\left(-\left(\frac{\Delta t}{\tau_+}\right)\right)\ [\%]\ (\Delta\ t> 0), \tag{5}$$

where the ΔW_{0-} and ΔW_{0+} are the ΔW at the Δt = 0 s and the τ_- and τ_+ are mean response times, respectively. The lines of Fig. 5(c) and (d) show that the STDP characteristics observed in our samples are well fitted with the synaptic strength-based model. The [$\Delta W_{0-}/\tau_-$, $\Delta W_{0+}/\tau_+$] parameters are extracted to be [90%/0.35 ms, −25%/0.35 ms]/[200%/0.25 ms, −35%/0.25 ms] in oxygen-poor/-rich samples. Consequently, the STDP in Pt/$LaAlO_3$/Nb-doped $SrTiO_3$ memristors becomes less sensitive to Δt as the P_{O2} becomes lower. Therefore, the trade-off between the large current and efficient STDP is clearly observed and it can be optimized by tuning P_{O2} depending on the neuromorphic applications.

Finally, the extracted STDP parameters are summarized in Table 1, in comparison with previous works. Our results prove that the Pt/$LaAlO_3$/Nb-doped $SrTiO_3$ can improve the STDP efficiency further than previous reported materials.

5. Conclusion

The conduction mechanism and the effect of the oxygen-content of the $LaAlO_3$ layer on the synaptic behavior are investigated in the Pt/

Table 1
Extracted STDP parameters in comparison with previous works.

Memristor materials	ΔW_{0-}	t_{0-}	ΔW_{0+}	t_{0+}	Year
MEH-PPV (Polymer) [24]	31.5%	4.16 ms	−13%	5.35 ms	2010
Ag + Si [10]	~15%	~50 ms	~ −30%	~40 ms	2010
TiO_x [25]	~ −5%	~70 ms	~12%	~100 ms	2011
InGaZnO [11]	~100%	~50 ms	~ −100%	~50 ms	2012
$Ge_2Sb_2Te_5$ [12]	~ −6%	~0.2 µs	~4%	~0.2 µs	2013
$LaAlO_3$/Nb-doped $SrTiO_3$ (Low P_{O2} in $LaAlO_3$)	90%	0.35 ms	−25%	0.35 ms	2017 (This work)
$LaAlO_3$/Nb-doped $SrTiO_3$ (High P_{O2} in $LaAlO_3$)	200 %	0.25 ms	−35 %	0.25 ms	2017 (This work)

$LaAlO_3$/Nb-doped $SrTiO_3$ memristor for neuromorphic applications. The conduction mechanism is well explained by the combination of the thermionic emission and P-F hopping associated with the V_O in the $LaAlO_3$ layer. As the oxygen-content decreases, the current becomes larger and the STDP becomes less sensitive to Δt, i.e., the degradation of STDP efficiency. It is found that the trade-off between large current and efficient STDP can be controlled by the oxygen-content. Furthermore, we prove that the Pt/$LaAlO_3$/Nb-doped $SrTiO_3$ can improve the STDP efficiency compared with previously reported memristor materials by extracting the synaptic strength-based model parameters. Our results suggest that the V_O-controlled perovskite material-based memristors are potentially promising candidates for synaptic devices in neuromorphic computing system.

Acknowledgement

This work was supported by the National Research Foundation of Korea (NRF) Grant funded by the Korean Government (MSIP) under Grant 2016R1A5A1012966, in part by the Ministry of Science, ICT and Future Planning Grant 2016M3A7B4909668, and in part by the Ministry of Science, ICT & Future Planning Grant 2011-0030230. C.Y., S. L., and B.H.P. were supported by the National Research Foundation of Korea (NRF) grants funded by the Korea government (MSIP) (No. 2013R1A3A2042120).

References

[1] Ohtomo A, Hwang HY. A high-mobility electron gas at the $LaAlO_3/SrTiO_3$ heterointerface. Nature 2004;427(29):423.
[2] Caviglia AD, Gariglio S, Reyren N, Jaccard D, Chneider T, Gabay M, et al. Electric field control of the $LaAlO_3/SrTiO_3$ interface ground state. Nature Lett 2008;456(4):624.
[3] Huijbe M, Brinkman A, Koster G, Rijnders G, Hilgenkamp H, Black DHA. Structure-property relation of $SrTiO_3/LaAlO_3$ interfaces. Adv Mater 2009;21:1665.
[4] Singh-Bhalla G, Bell C, Ravichandran J, Siemons W, Hikita Y, Salahuddin S, et al. Built-in and induced polarization across $LaAlO_3/SrTiO_3$ heterojunctions. Nature Phys 2011;7:80.
[5] Kalabukhov A, Gunnarsson R, Borjesson J, Olsson E, Claeson T, Winkler D. Effect of oxygen vacancies in the SrTiO3 substrate on the electrical properties of the $LaAlO_3/SrTiO_3$ interface. Phys Rev B 2011;75(12):121404.
[6] Nakagawa N, Hwang HY, Muller DA. Why some interfaces cannot be sharp. Nature Mater 2006;5:204.
[7] Wu S, Ren L, Qing J, Yu F, Yang K, Yang M, et al. Bipolar resistance switching in transparent ITO/$LaAlO_3/SrTiO_3$ memristors. ACS Appl Mater Interface 2014;6:8575.
[8] Wu S, Luo X, Turner S, Peng H, Lin W, Ding J, et al. Nonvolatile resistive switching in Pt/$LaAlO_3/SrTiO_3$ heterostructures. Phys Rev X 2013;3(4):041027.
[9] Kim H, Chan NY, Dai J, Kim D-W. Enhanced surface-and interface coupling in Pd-nanoparticle-coated $LaAlO_3/SrTiO_3$ heterostructures: strong gas- and photo-induced conductance modulation. Sci Rep 2015;5:8531.
[10] Jo SH, Chang T, Ebong I, Bhadviya BB, Mazumder P, Lu W. Nanoscale memristor device as synapse in neuromorphic systems. Nano Lett 2010;10:1297.
[11] Wang ZQ, Xu HY, Li XH, Yu H, Liu YC, Zhu XJ. Synaptic learning and memory functions achieved using oxygen ion migration/diffusion in an amorphous InGaZnO memristor. Adv Func Mater 2012;22:2759.
[12] Li Y, Zhong Y, Xu L, Zhang J, Xu X, Sun H, et al. Ultrafast synaptic events in a chalcogenide memristor. Sci Rep 2013;3:1619.
[13] Park S, Kim H, Choo M, Noh J, Sheri A, Jung S, et al. RRAM-based synapse for neuromorphic system with pattern recognition function. IEDM Tech Dig 2012;231.
[14] Kim S, Du C, Sheridan P, Ma W, Choi SH, Lu W. Experimental demonstration of a second-order memristor and its ability to biorealistically implement synaptic plasticity. Nano Lett 2015;15:2203.
[15] Kim TH, Jang EY, Lee NJ, Choi DJ, Lee K-J, Jang J-T, et al. Nanoparticle assemblies as memristors. Nano Lett 2009;9(6):2229.
[16] Kim M-S, Hwang YH, Ki S, Guo Z, Moon D-I, Choi J-M, et al. Effects of the oxygen vacancy concentration in InGaZnO-based resistance random access memory. Appl Phys Lett 2012;101:243503.
[17] Nili H, Walia S, Balendhran S, Strukov DB, Bhaskaran M, Sriram S. Nanoscale resistive switching in amorphous perovskite oxide (a-$SrTiO_3$) memristors. Adv Func Mater 2014;24:6741.
[18] Wu S, Ren L, Yu F, Yang K, Yang M, Wang Y, et al. Colossal resistance switching in Pt/$BiFeO_3$/Nb:$SrTiO_3$ memristor. S Appl Phys A 2014;116:1741.
[19] Ahrens M, Merkle R, Rahmati B, Maier J. Effective masses of electrons in n-type $SrTiO_3$ determined from low-temperature specific heat capacities. Phys B 2007;393:239.
[20] Ohta S, Nomura T, Ohta H, Koumoto K. High-temperature carrier transport and thermoelectric properties of heavily La- or Nb-doped $SrTiO_3$ single crystals. J Appl Phys 2005;97:034106.
[21] Liu K-C, Tzeng W-H, Chang K-M, Huang J-J, Lee Y-J, Yeh P-H, et al. Investigation of the effect of different oxygen partial pressure to $LaAlO_3$ thin film properties and resistive switching characteristics. Thin Solid Films 2011;520:1246.
[22] Mitra C, Lin C, Roberson J, Demkov AA. Electronic structure of oxygen vacancies in $SrTiO_3$ and $LaAlO_3$. Phys Rev B 2012;86:155105.
[23] Bi G, Poo M. Synaptic modifications in cultured hippocampal neurons: dependence on spike timing, synaptic strength, and postsynaptic cell type. J Neurosci 1998;18(24):10464.
[24] Lai Q, Zhang L, Li Z, Stickle WF, Williams RS, Chen Y. Ionic/electronic hybrid materials integrated in a synaptic transistor with signal processing and learning functions. Adv Mater 2010;22:2448.
[25] Seo K, Kim I, Jung S, Jo M, Park S, Park J, et al. Analog memory and spike-timing-dependent plasticity characteristics of a nanoscale titanium oxide bilayer resistive switching device. Nanotechology 2011;22:254023.